Available online at www.sciencedirect.com
SCIENCE DIRECT®
International Journal of Heat and Mass Transfer 47 (2004) 1201–1215
International Journal of HEAT and MASS TRANSFER
www.elsevier.com/locate/ijhmt

Inverse natural convection problem of simultaneous estimation of two boundary heat fluxes in irregular cavities

Marcelo J. Colaço, Helcio R.B. Orlande *

Department of Mechanical Engineering—EE/COPPE, Federal University of Rio de Janeiro, UFRJ, Cx. Postal: 68503, Rio de Janeiro 21945-970, Brazil

Received 10 May 2003; received in revised form 12 September 2003

Abstract

This paper deals with the use of the Conjugate Gradient Method of function estimation with Adjoint Problem for the simultaneous identification of two boundary conditions in natural convection inverse problems in two-dimensional irregular cavities. The unknown boundary conditions are estimated with no a priori information about their functional forms. Irregular geometries in the physical domain are transformed into regular geometries in the computational domain by using an elliptic scheme of numerical grid generation. Therefore, the proposed formulation can be applied to the solution of inverse problems in different geometries. The methodology is applied to cases involving an annular cavity, where the position- and time-dependent heat fluxes are unknown at the inner and outer surfaces. The effects of the number and position of temperature sensors on the inverse problem solution are also addressed in the paper.

Keywords: Inverse problem; Natural convection; Conjugate gradient method; Adjoint operator

1. Introduction

Forced and natural convection problems have been gaining the attention of groups aiming at the development of solution procedures for inverse problems, as well as of groups mainly involved with the physical/application aspects of this class of problems. Several recent works dealing with inverse convection problems can be found in Refs. [1–33]. However, with few exceptions [26–28,30], the above papers have addressed the estimation of one single unknown quantity.

The use of simulated measurements has been widely used to verify the capabilities of inverse problem solution procedures [1–35]. In such approach, the direct problem is solved with a priori established values for the unknown parameters or functions. The solution of the direct problem then provides *exact* measurements to be used as input data for the inverse problem solution procedure. Note, however, that actual measurements generally contain errors. Therefore, in order to simulate actual measured data, random errors are added to the *exact* measurements. Standard statistical hypotheses generally assumed for the measurement errors include they being regarded as additive, uncorrelated, normally distributed, with zero mean and with constant and known standard deviation [33–35]. By using simulated measurements obtained in such a manner, the inverse problem solution procedure shall be able to recover the values a priori established for the unknown parameters or functions. Different important issues can then be addressed with the use of simulated measurements, such as the stability of the solution procedure with respect to the measurement errors, as well as the design of the experiment, including the estimation of the number and position of sensors required for accurate inverse problem solutions.

A fact usually overlooked when simulated measurements are used for the inverse analysis is that the errors in the mathematical model for the physical problem under picture, as well as in the solution technique for the direct problem, are neglected. Such is the case because

* Corresponding author.
E-mail addresses: colaco@ufrj.br (M.J. Colaço), helcio@serv.com.ufrj.br (H.R.B. Orlande).

0017-9310/$ - see front matter © 2003 Elsevier Ltd. All rights reserved.
doi:10.1016/j.ijheatmasstransfer.2003.09.007

Nomenclature

C_p	specific heat
d	direction of descent
F	objective functional
K	thermal conductivity
M, N	number of grid lines in the ξ and η directions, respectively
P	pressure
q_1, q_2	applied heat fluxes at the boundaries $\eta = 1$ and $\eta = N$, respectively
S	number of sensors
$\mathbf{S}^{\phi}$	vector of source functions given by Eq. (3c)
t	time
t_f	final time
T	estimated temperature
u, v	velocity components in x and y directions, respectively
$\widetilde{U}$, $\widetilde{V}$	contravariant velocity components normal to ξ and η coordinate lines, respectively
x, y	Cartesian coordinates in the physical domain

Greek symbols

β	search step size
Δ	variation
ε_{RMS}	RMS error
γ, χ	conjugation coefficients
$\mathbf{\Gamma}^{\phi}$	vector of diffusion coefficients given by Eq. (3b)
$\boldsymbol{\varphi}$	vector of conserved variables given by Eq. (3a)
$\boldsymbol{\lambda}$	vector of Lagrange multipliers given by Eq. (9)
μ_s	measured temperature by sensor s
ρ	density
σ	standard deviation of the measurement errors
ξ, η	Cartesian coordinates in the computational domain
μ	dynamic viscosity
∇F	gradient of the objective functional

Subscripts

est, ex	estimated and exact heat fluxes
s	sensor location
1, 2	refer to the boundaries at $\eta = 1$ and $\eta = N$, respectively

Superscript

k	iteration number

the mathematical formulation and the solution technique for the direct problem, used to generate the simulated measurements, are the same used as part of the inverse problem solution procedure. In fact, for solving the inverse problem and for generating the simulated measurements, many analysts solve the direct problem disregarding the accuracy of its solution, which can result in unrealistic simulated measurements that may not be identified through the inverse analysis.

In this paper, we examine the simultaneous estimation of the boundary heat fluxes at two surfaces of a cavity, by using simulated temperature measurements taken in its interior. The fluid inside the cavity undergoes natural convection as a result of the prescribed boundary conditions. The natural convection problem is formulated in terms of generalized boundary-fitted coordinates [36], by using Boussinesq's approximation. The irregular geometry in the physical domain is transformed into a regular geometry in the computational domain, so that one single formulation can be used for the solution of inverse problems in cavities of different geometries. For the solution of the inverse problem, we consider the conjugate gradient method of function estimation with adjoint problem [34,35]. The direct problem and the auxiliary problems required by this method are numerically solved with finite-volumes, by utilizing the WUDS [37] interpolation scheme. The SIMPLEC method [38] was utilized for the treatment of the pressure–velocity coupling, for the computation of the velocity and pressure fields on co-located grids. Test-cases involving the simultaneous estimation of the heat fluxes at the inner and outer surfaces of an annular cavity are examined. The most general case, where the unknown heat fluxes vary in time and along the boundary surfaces, is addressed below.

2. Physical problem and mathematical formulation

The physical problem under picture in this paper involves the transient laminar natural convection of a fluid inside a two-dimensional irregular cavity, such as the one depicted in Fig. 1. The boundary of the cavity is assumed to be defined by four surfaces, which are transformed into the computational domain as the surfaces $\xi = 1$, $\xi = M$, $\eta = 1$ and $\eta = N$. The fluid is initially at rest and at the uniform temperature T_c. At time zero, the surfaces at $\eta = 1$ and at $\eta = N$ are subjected to space- and time-dependent heat fluxes $q_1(\xi, t)$ and $q_2(\xi, t)$, respectively. The other two surfaces involve

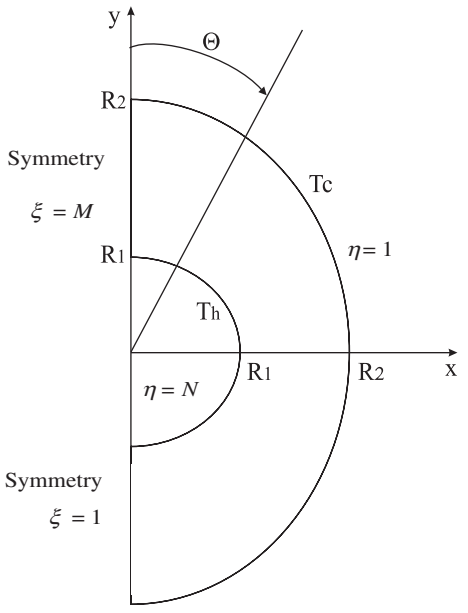

Fig. 1. Geometry for the irregular cavity.

symmetry boundary conditions. The fluid properties are assumed constant, except for the density in the buoyancy term, where we consider Boussinesq's approximation valid.

The mathematical formulation for this physical problem can be written in vector form in terms of the following conservation equation in the generalized Cartesian coordinates:

$$\frac{\partial(J\rho\boldsymbol{\varphi})}{\partial t}+\frac{\partial(\widetilde{U}\rho\boldsymbol{\varphi})}{\partial\xi}+\frac{\partial(\widetilde{V}\rho\boldsymbol{\varphi})}{\partial\eta} = \frac{\partial}{\partial\xi}\left\{J\boldsymbol{\Gamma}^{\phi}\left[a\frac{\partial\boldsymbol{\varphi}}{\partial\xi}+d\frac{\partial\boldsymbol{\varphi}}{\partial\eta}\right]\right\} + \frac{\partial}{\partial\eta}\left\{J\boldsymbol{\Gamma}^{\phi}\left[d\frac{\partial\boldsymbol{\varphi}}{\partial\xi}+b\frac{\partial\boldsymbol{\varphi}}{\partial\eta}\right]\right\}+J\mathbf{S}^{\phi} \tag{1}$$

where

$$a=\xi_x^2+\xi_y^2;\quad b=\eta_x^2+\eta_y^2;$$

$$d=\xi_x\eta_x+\xi_y\eta_y;\quad J=x_\xi y_\eta-x_\eta y_\xi;$$

$$\widetilde{U}=J(u\xi_x+v\xi_y);\quad \widetilde{V}=J(u\eta_x+v\eta_y) \tag{2a–f}$$

We note that $\widetilde{U}$ and $\widetilde{V}$ denote the contravariant velocities in the ξ and η directions, respectively, while J defines the Jacobian of the transformation from the physical domain into the computational domain. The general conservation variable, as well as the diffusion coefficient and the source term for the mass, momentum and energy conservation equations, are given in vector form respectively as:

$$\boldsymbol{\varphi}=\begin{bmatrix}1\\ u(\xi,\eta,t)\\ v(\xi,\eta,t)\\ T(\xi,\eta,t)\end{bmatrix},\quad \boldsymbol{\Gamma}^{\phi}=\begin{bmatrix}0&0&0&0\\0&\mu&0&0\\0&0&\mu&0\\0&0&0&\frac{K}{C_p}\end{bmatrix},$$

$$\mathbf{S}^{\phi}=\begin{bmatrix}0\\ -\dfrac{\partial P(\xi,\eta,t)}{\partial x}\\ -\dfrac{\partial P(\xi,\eta,t)}{\partial y}-\rho g\{1-\beta[T(\xi,\eta,t)-T_{\mathrm{ref}}]\}\\ 0\end{bmatrix} \tag{3a–c}$$

We note in the Eq. (3c) that the positive y-axis in the physical domain is supposed to be aligned with the opposite direction of the gravitational acceleration vector. These equations are solved, subjected to the following boundary and initial conditions.

$$J\boldsymbol{\Gamma}^{\phi}\left[a\frac{\partial\boldsymbol{\varphi}}{\partial\xi}+b\frac{\partial\boldsymbol{\varphi}}{\partial\eta}\right]=0\quad \text{at } \xi=1 \text{ and } \xi=M,\quad 1<\eta<N,\ \text{for } t>0 \tag{4a}$$

$$u=v=0\quad \text{at } \eta=1 \text{ and } \eta=N,\quad 1<\xi<M,\ \text{for } t>0 \tag{4b}$$

$$K\left[d\frac{\partial T}{\partial\xi}+b\frac{\partial T}{\partial\eta}\right]=-q_1(\xi,t)\sqrt{b}\quad \text{at } \eta=1,\ 1<\xi<M,\ \text{for } t>0 \tag{4c}$$

$$K\left[d\frac{\partial T}{\partial\xi}+b\frac{\partial T}{\partial\eta}\right]=q_2(\xi,t)\sqrt{b}\quad \text{at } \eta=N,\ 1<\xi<M,\ \text{for } t>0 \tag{4d}$$

$$u=v=0\quad \text{for } t=0 \text{ in the region} \tag{4e}$$

$$T=T_{\mathrm{c}}\quad \text{for } t=0 \text{ in the region} \tag{4f}$$

3. Direct problem and inverse problem

The *direct problem* associated with the mathematical formulation given by Eqs. (1)–(4) involves the determination of the transient velocity and temperature fields in the cavity, from the knowledge of the cavity geometry, of the physical properties and of the initial and boundary conditions. Appropriately formulated direct problems are mathematically classified as *well-posed*. The solution of a well-posed problem must satisfy the conditions of existence, uniqueness and stability with respect to the input data [33–35].

Inverse heat transfer problems involve the estimation of at least one of the quantities required for the well-posedness of the direct problem, by using velocity, heat flux and/or temperature measurements. The *inverse*

problem of interest in this work involves the simultaneous estimation of the boundary heat fluxes $q_1(\xi,t)$ and $q_2(\xi,t)$, at the surfaces $\eta=1$ and $\eta=N$, respectively. Temperature measurements taken inside the cavity at appropriate locations are used for the estimation of such boundary fluxes.

Differently from direct problems, inverse problems are mathematically classified as *Ill-posed*. The existence of a solution for an inverse heat transfer problem may be assured by physical reasoning for several cases. On the other hand, the uniqueness of the solution of inverse problems can be mathematically proved only for some special cases. Also, the inverse problem is very sensitive to random errors in the measured input data, thus requiring special techniques for its solution in order to satisfy the stability condition [33–35]. In fact, a successful solution of an inverse problem generally involves its reformulation as an approximate well-posed problem and makes use of some kind of regularization (stabilization) technique. In several methods, the solution for the inverse problem is obtained through the minimization of an L_2 norm in the space where the unknown quantity belongs to. For the solution of the inverse problem under picture in this work we consider the minimization of the following functional:

$$F[q_1(\xi,t),q_2(\xi,t)] = \frac{1}{2}\int_{t=0}^{t_f}\sum_{s=1}^{S}[T(\xi_s,\eta_s,t;q_1,q_2)-\mu_s(t)]^2\,\mathrm{d}t \tag{5}$$

where t_f denotes the final time, S is the number of sensors used in the analysis, while $\mu_s(t)$ and $T(\xi_s,\eta_s,t;q_1,q_2)$ are the measured and estimated temperatures, respectively, at the measurement positions (ξ_s,η_s), for $s=1,\ldots,S$. The estimated temperatures are obtained from the solution of the direct problem by using estimates for the boundary heat fluxes $q_1(\xi,t)$ and $q_2(\xi,t)$.

We note that the physical problem under picture involves transient natural convection with the surfaces at $\eta=1$ and $\eta=N$ subjected to heat fluxes $q_1(\xi,t)$ and $q_2(\xi,t)$. The recovery of this type of functions *via* inverse analysis requires transient measurements taken at several locations inside the cavity.

4. Sensitivity problems

The sensitivity problem is used to determine the variation of the dependent variables due to changes in the unknown quantity. Since the present work deals with the estimation of two unknown functions, two sensitivity problems are required in the analysis. They are derived by considering perturbations in the boundary heat fluxes each at a time, as described next.

Let us consider that the temperature $T(\xi,\eta,t)$ undergoes a variation $\varepsilon\Delta T_1(\xi,\eta,t)$, when the boundary heat flux $q_1(\xi,t)$ is perturbed by $\varepsilon\Delta q_1(\xi,t)$, where ε is a small real number. Similarly, since the temperature, velocities and pressure are coupled in the natural convection problem, the velocities and the pressure undergo variations $\varepsilon\Delta u_1(\xi,\eta,t)$, $\varepsilon\Delta v_1(\xi,\eta,t)$ and $\varepsilon\Delta P_1(\xi,\eta,t)$. In order to derive the sensitivity problem resulting from the perturbation in $q_1(\xi,t)$, we apply the following limiting process [34,35]:

$$D_{\Delta q_1}T(\xi,\eta,t)=\lim_{\varepsilon\to 0}\frac{L_\varepsilon(q_{1\varepsilon})-L(q_1)}{\varepsilon}=0 \tag{6}$$

where $L_\varepsilon(q_{1\varepsilon})$ and $L(q_1)$ are the operator forms of the direct problem written for the perturbed $[q_1(\xi,t)+\varepsilon\Delta q_1(\xi,t)]$ and unperturbed $q_1(\xi,t)$ heat fluxes at the boundary $\eta=1$, respectively.

A similar procedure is used for the derivation of the sensitivity problem for the functions $\Delta T_2(\xi,\eta,t)$, $\Delta u_2(\xi,\eta,t)$, $\Delta v_2(\xi,\eta,t)$ and $\Delta P_2(\xi,\eta,t)$, resultant from the perturbation of the heat flux $q_2(\xi,t)$ by $\varepsilon\Delta q_2(\xi,t)$, at the boundary $\eta=N$.

We then obtain the sensitivity problems for the determination of the functions $\Delta\boldsymbol{\varphi}_j(\xi,\eta,t)$, for $j=1,\ 2$, respectively as:

$$\begin{aligned}&\frac{\partial(J\rho\Delta\boldsymbol{\varphi}_j)}{\partial t}+\frac{\partial(\widetilde{U}_j\rho\Delta\boldsymbol{\varphi}_j)}{\partial\xi}+\frac{\partial(\widetilde{V}_j\rho\Delta\boldsymbol{\varphi}_j)}{\partial\eta}+\frac{\partial(\Delta\widetilde{U}_j\rho\boldsymbol{\varphi}_j)}{\partial\xi}\\&\quad+\frac{\partial(\Delta\widetilde{V}_j\rho\boldsymbol{\varphi}_j)}{\partial\eta}\\&\quad=\frac{\partial}{\partial\xi}\left\{J\boldsymbol{\Gamma}^{\phi}\left[a\frac{\partial(\Delta\boldsymbol{\varphi}_j)}{\partial\xi}+d\frac{\partial(\Delta\boldsymbol{\varphi}_j)}{\partial\eta}\right]\right\}\\&\qquad+\frac{\partial}{\partial\eta}\left\{J\boldsymbol{\Gamma}^{\phi}\left[d\frac{\partial(\Delta\boldsymbol{\varphi}_j)}{\partial\xi}+b\frac{\partial(\Delta\boldsymbol{\varphi}_j)}{\partial\eta}\right]\right\}+J\Delta\mathbf{S}_j^{\phi}\\&\quad\text{in } 1<\xi<M,\ 1<\eta<N;\ \text{for } t>0\end{aligned} \tag{7a}$$

$$\begin{aligned}&J\boldsymbol{\Gamma}^{\phi}\left[a\frac{\partial(\Delta\boldsymbol{\varphi}_j)}{\partial\xi}+b\frac{\partial(\Delta\boldsymbol{\varphi}_j)}{\partial\eta}\right]=0\\&\quad\text{at } \xi=1 \text{ and } \xi=M,\ 1<\eta<N,\ \text{for } t>0\end{aligned} \tag{7b}$$

$$\begin{aligned}&\Delta u_j=\Delta v_j=0\quad\text{at } \eta=1 \text{ and}\\&\quad\eta=N,\ 1<\xi<M,\ \text{for } t>0\end{aligned} \tag{7c}$$

$$\begin{aligned}&K\left[d\frac{\partial(\Delta T_j)}{\partial\xi}+b\frac{\partial(\Delta T_j)}{\partial\eta}\right]=-\delta_{1j}\Delta q_1(\xi,t)\sqrt{b}\\&\quad\text{at } \eta=1,\ 1<\xi<M,\ \text{for } t>0\end{aligned} \tag{7d}$$

$$\begin{aligned}&K\left[d\frac{\partial(\Delta T_j)}{\partial\xi}+b\frac{\partial(\Delta T_j)}{\partial\eta}\right]=\delta_{2j}\Delta q_2(\xi,t)\sqrt{b}\\&\quad\text{at } \eta=N,\ 1<\xi<M,\ \text{for } t>0\end{aligned} \tag{7e}$$

$$\Delta\boldsymbol{\varphi}=0\quad\text{for } t=0 \text{ in the region} \tag{7f}$$

where $\boldsymbol{\varphi}$, $\boldsymbol{\Gamma}$ and $\mathbf{S}^{\phi}$ are given by Eqs. (3a–c), respectively and

$$\delta_{ij} = \begin{cases} 0, & \text{for } i \neq j \\ 1, & \text{for } i = j \end{cases} \tag{8}$$

Note in Eqs. (3a–c) and (7a) that the correspondent of the energy and y-momentum equations for the sensitivity problems are coupled through the variation of the buoyancy term. Thus, for the sensitivity problems the mass, x-momentum, y-momentum and energy equations must be solved simultaneously, for $j = 1, 2$.

5. Adjoint problem

The adjoint problem is derived by multiplying the general conservation Eq. (1) written for $\boldsymbol{\varphi} \equiv 1$ (mass equation) by the *Lagrange multiplier* $\lambda_1(\xi,\eta,t)$, Eq. (1) written for $\boldsymbol{\varphi} \equiv u(\xi,\eta,t)$ (x-momentum equation) by the *Lagrange multiplier* $\lambda_2(\xi,\eta,t)$, Eq. (1) written for $\boldsymbol{\varphi} \equiv v(\xi,\eta,t)$ (y-momentum equation) by the *Lagrange multiplier* $\lambda_3(\xi,\eta,t)$, Eq. (1) written for $\boldsymbol{\varphi} \equiv T(\xi,\eta,t)$ (energy equation) by the *Lagrange multiplier* $\lambda_4(\xi,\eta,t)$ and integrating over the time and space domains. The resulting expression is then added to the functional given by Eq. (5) in order to obtain an extended functional. Then, by defining the Lagrange multiplier vector as

$$\boldsymbol{\lambda} = \begin{bmatrix} \lambda_1(\xi,\eta,t) \\ \lambda_2(\xi,\eta,t) \\ \lambda_3(\xi,\eta,t) \\ \lambda_4(\xi,\eta,t) \end{bmatrix} \tag{9}$$

we can write the extended functional as:

$$\begin{aligned} &F[q_1(\xi,t), q_2(\xi,t)] \\ &= \frac{1}{2}\int_{\xi=1}^{M}\int_{\eta=1}^{N}\int_{t=0}^{t_f}\sum_{s=1}^{S}(T_s-\mu_s)^2\delta(\mathbf{r}-\mathbf{r}_s)\,\mathrm{d}t\,\mathrm{d}\eta\,\mathrm{d}\xi \\ &\quad + \int_{\xi=1}^{M}\int_{\eta=1}^{N}\int_{t=0}^{t_f}\left\langle\left\{\frac{\partial(J\rho\boldsymbol{\varphi})}{\partial t}+\frac{\partial(\widetilde{U}\rho\boldsymbol{\varphi})}{\partial\xi}+\frac{\partial(\widetilde{V}\rho\boldsymbol{\varphi})}{\partial\eta}\right.\right. \\ &\quad -\frac{\partial}{\partial\xi}\left[J\boldsymbol{\Gamma}^{\phi}\left(a\frac{\partial\boldsymbol{\varphi}}{\partial\xi}+d\frac{\partial\boldsymbol{\varphi}}{\partial\eta}\right)\right] \\ &\quad \left.\left.-\frac{\partial}{\partial\eta}\left[J\boldsymbol{\Gamma}^{\phi}\left(d\frac{\partial\boldsymbol{\varphi}}{\partial\xi}+b\frac{\partial\boldsymbol{\varphi}}{\partial\eta}\right)\right]-J\mathbf{S}^{\phi}\right\},\boldsymbol{\lambda}\right\rangle J\,\mathrm{d}t\,\mathrm{d}\eta\,\mathrm{d}\xi \end{aligned} \tag{10}$$

where $\delta(\cdot)$ is the Dirac delta function, $\mathbf{r}_s$ is the vector with the sensor position (ξ_s,η_s), for $s = 1,\ldots,S$ and $\langle .,. \rangle$ denotes the vector dot product.

We now perturb $q_1(\xi,t)$ by $\varepsilon\Delta q_1(\xi,t)$, $\boldsymbol{\varphi}(\xi,\eta,t)$ by $\varepsilon\Delta\boldsymbol{\varphi}_1(\xi,\eta,t)$ and $\mathbf{S}^{\phi}(\xi,\eta,t)$ by $\varepsilon\Delta\mathbf{S}_1^{\phi}(\xi,\eta,t)$ in Eq. (10) and apply the following limiting process to obtain the directional derivative of the functional $F[q_1(\xi,t), q_2(\xi,t)]$ in the direction of the perturbation $\Delta q_1(\xi,t)$ [34,35]:

$$D_{\Delta q_1}F[q_1(\xi,t),q_2(\xi,t)] = \lim_{\varepsilon\to 0}\frac{F_{\varepsilon}(q_{1\varepsilon})-F(q_1)}{\varepsilon} = 0 \tag{11}$$

where $F_{\varepsilon}(q_{1\varepsilon})$ and $F(q_1)$ denote the functional (10) written for the perturbed $[q_1(\xi,t)+\varepsilon\Delta q_1(\xi,t)]$ and unperturbed $q_1(\xi,t)$ heat fluxes at the boundary $\eta = 1$, respectively. The following expression results:

$$\begin{aligned} &D_{\Delta q_1}F[q_1(\xi,t),q_2(\xi,t)] \\ &= \int_{\xi=1}^{M}\int_{\eta=1}^{N}\int_{t=0}^{t_f}\sum_{s=1}^{S}(T_s-\mu_s)\delta(\mathbf{r}-\mathbf{r}_s)\Delta T_{1s}\,\mathrm{d}t\,\mathrm{d}\eta\,\mathrm{d}\xi \\ &\quad + \int_{\xi=1}^{M}\int_{\eta=1}^{N}\int_{t=0}^{t_f}\left\langle\left\{\frac{\partial(J\rho\Delta\boldsymbol{\varphi}_1)}{\partial t}+\frac{\partial(\widetilde{U}_1\rho\Delta\boldsymbol{\varphi}_1)}{\partial\xi}\right.\right. \\ &\quad +\frac{\partial(\widetilde{V}_1\rho\Delta\boldsymbol{\varphi}_1)}{\partial\eta}+\frac{\partial(\Delta\widetilde{U}_1\rho\boldsymbol{\varphi}_1)}{\partial\xi}+\frac{\partial(\Delta\widetilde{V}_1\rho\boldsymbol{\varphi}_1)}{\partial\eta} \\ &\quad -\frac{\partial}{\partial\xi}\left[J\boldsymbol{\Gamma}^{\phi}\left(a\frac{\partial(\Delta\boldsymbol{\varphi}_1)}{\partial\xi}+d\frac{\partial(\Delta\boldsymbol{\varphi}_1)}{\partial\eta}\right)\right] \\ &\quad -\frac{\partial}{\partial\eta}\left[J\boldsymbol{\Gamma}^{\phi}\left(d\frac{\partial(\Delta\boldsymbol{\varphi}_1)}{\partial\xi}+b\frac{\partial(\Delta\boldsymbol{\varphi}_1)}{\partial\eta}\right)\right] \\ &\quad \left.\left.-J\Delta\mathbf{S}_1\right\},\boldsymbol{\lambda}\right\rangle J\,\mathrm{d}t\,\mathrm{d}\eta\,\mathrm{d}\xi \end{aligned} \tag{12}$$

By employing integration by parts in the second integral term appearing on the right-hand side of Eq. (12), utilizing the initial and boundary conditions of the sensitivity problem for $\Delta T_1(\xi,\eta,t)$ and also requiring that the coefficients of $\Delta T_1(\xi,\eta,t)$ in the resulting equation vanish, the following *adjoint problem* is obtained:

$$\begin{aligned} &-\frac{\partial(J^2\rho\boldsymbol{\psi})}{\partial t}-\frac{\partial(\widetilde{U}\rho\boldsymbol{\psi}J)}{\partial\xi}-\frac{\partial(\widetilde{V}\rho\boldsymbol{\psi}J)}{\partial\eta} \\ &\quad = \frac{\partial}{\partial\xi}\left\{J\boldsymbol{\Gamma}^{\phi}\left[a\frac{\partial(\boldsymbol{\psi}J)}{\partial\xi}+d\frac{\partial(\boldsymbol{\psi}J)}{\partial\eta}\right]\right\} \\ &\quad\quad +\frac{\partial}{\partial\eta}\left\{J\boldsymbol{\Gamma}^{\phi}\left[d\frac{\partial(\boldsymbol{\psi}J)}{\partial\xi}+b\frac{\partial(\boldsymbol{\psi}J)}{\partial\eta}\right]\right\}+\mathbf{S}_{\lambda}^{\phi} \\ &\quad \text{in } 1<\xi<M,\ 1<\eta<N;\ \text{for } t<t_f \end{aligned} \tag{13a}$$

$$\begin{aligned} &J\boldsymbol{\Gamma}^{\phi}\left[a\frac{\partial(\boldsymbol{\psi}J)}{\partial\xi}+b\frac{\partial(\boldsymbol{\psi}J)}{\partial\eta}\right]=0 \\ &\quad \text{at } \xi=1 \text{ and } \xi=M,\ 1<\eta<N,\ \text{for } t>0 \end{aligned} \tag{13b}$$

$$\begin{aligned} &\lambda_2=\lambda_3=0 \\ &\quad \text{at } \eta=1 \text{ and } \eta=N,\ 1<\xi<M,\ \text{for } t>0 \end{aligned} \tag{13c}$$

$$\begin{aligned} &JK\left[d\frac{\partial\lambda_4}{\partial\xi}+b\frac{\partial\lambda_4}{\partial\eta}\right]=0 \quad \text{at } \eta=1 \text{ and} \\ &\quad \eta=N,\ 1<\xi<M,\ \text{for } t>0 \end{aligned} \tag{13d}$$

$$\boldsymbol{\psi}=0 \quad \text{for } t=t_f \text{ in the region} \tag{13e}$$

where

$$\mathbf{S}_{\lambda}^{\phi}=\begin{pmatrix} \dfrac{\partial \widetilde{U}_{\lambda}}{\partial \xi}+\dfrac{\partial \widetilde{V}_{\lambda}}{\partial \eta} \\ -J\dfrac{\partial(\lambda_1 J)}{\partial x}+\left\langle \boldsymbol{\varphi},\left[\dfrac{\partial(\rho\boldsymbol{\psi}J^2\xi_x)}{\partial \xi}+\dfrac{\partial(\rho\boldsymbol{\psi}J^2\eta_x)}{\partial \eta}\right]\right\rangle \\ -J\dfrac{\partial(\lambda_1 J)}{\partial y}+\left\langle \boldsymbol{\varphi},\left[\dfrac{\partial(\rho\boldsymbol{\psi}J^2\xi_x)}{\partial \xi}+\dfrac{\partial(\rho\boldsymbol{\psi}J^2\eta_x)}{\partial \eta}\right]\right\rangle \\ \rho g\beta\lambda_3 J^2-\sum_{s=1}^{S}(T_s-\mu_s)\delta(\mathbf{r}-\mathbf{r}_s) \end{pmatrix},$$

$$\boldsymbol{\psi}=\begin{pmatrix} 0 \\ \lambda_2(\xi,\eta,t) \\ \lambda_3(\xi,\eta,t) \\ \lambda_4(\xi,\eta,t) \end{pmatrix} \tag{14a, b}$$

and

$$\widetilde{U}_{\lambda}=J^2(\lambda_2\xi_x+\lambda_3\xi_y) \tag{15a}$$

$$\widetilde{V}_{\lambda}=J^2(\lambda_2\eta_x+\lambda_3\eta_y) \tag{15b}$$

are the contravariant components of the Lagrange multipliers $\lambda_2(\xi,\eta,t)$ and $\lambda_3(\xi,\eta,t)$ multiplied by the Jacobian.

Note that the Lagrange multiplier $\lambda_1(\xi,\eta,t)$ appears in the second and third components of the source term vector $\mathbf{S}_{\lambda}$, just like the pressure appears in the source term of the x and y-momentum equations. Similarly, the Lagrange multipliers $\lambda_2(\xi,\eta,t)$ and $\lambda_3(\xi,\eta,t)$ are equivalent to the u and v velocity components, while the Lagrange multiplier $\lambda_4(\xi,\eta,t)$ is equivalent to the temperature in the energy equation. Therefore, the adjoint problem given by Eqs. (13)–(15) is also coupled and needs to be solved with the same technique used for the direct problem.

We note that the adjoint problem involves final conditions given by Eq. (13e) (instead of the usual initial conditions), as well as negative transient and convective terms in the governing Eq. (13a). However, it can be transformed into a regular problem by utilizing the following suitable transformations of the independent variables:

$$\xi^*=M-\xi,\quad \eta^*=N-\eta,\quad t^*=t_{\mathrm{f}}-t \tag{16a–c}$$

A limiting process analogous to Eq. (11) is used in order to obtain the directional derivative of the functional $F[q_1(\xi,t),q_2(\xi,t)]$ in the direction of the perturbation $\Delta q_2(\xi t)$ [34,35]. After performing similar manipulations we obtain the adjoint problem resulting from the perturbation in $q_2(\xi,t)$, which is identical to that given by Eqs. (13)–(15) resulting from the perturbation in $q_1(\xi,t)$. Therefore, one single adjoint problem needs to be solved at each iteration of the conjugate gradient method, despite the fact that two unknown functions are to be estimated.

6. Gradient equations

In the process of obtaining the adjoint problem resulting from the perturbation in $q_1(\xi,t)$, the directional derivative of the functional in the direction $\Delta q_1(\xi,t)$ reduces to

$$D_{\Delta q_1}F[q_1(\xi,t),q_2(\xi,t)] = -\int_{\xi=1}^{M}\int_{t=0}^{t_{\mathrm{f}}}\left[\frac{\sqrt{b}}{C_p}J^2\lambda_4(\xi,\eta,t)\right]_{\eta=1}\Delta q_1(\xi,t)\,\mathrm{d}t\,\mathrm{d}\xi \tag{17}$$

We now invoke the hypothesis that the unknown functions belong to the space of square integrable functions in the domain $]0,t_{\mathrm{f}}[\times]1,M[$ of interest. The directional derivative of $F[q_1(\xi,t),q_2(\xi,t)]$ in the direction of the perturbation $\Delta q_1(\xi,t)$ is given by [34–36]:

$$D_{\Delta q_1}F[q_1(\xi,t),q_2(\xi,t)] = \int_{\xi=1}^{M}\int_{t=0}^{t_{\mathrm{f}}}\nabla F[q_1(\xi,t)]\Delta q_1(\xi,t)\sqrt{b}J\,\mathrm{d}t\,\mathrm{d}\xi \tag{18a}$$

Hence, by comparing Eqs. (17) and (18a), we obtain the gradient equation for the estimation of $q_1(\xi,t)$ as:

$$\nabla F[q_1(\xi,t)] = -\left.\frac{J\lambda_4(\xi,\eta,t)}{C_p}\right|_{\eta=1} \tag{18b}$$

An analogous procedure is used in order to obtain the gradient equation of the functional for the estimation of the function $q_2(\xi,t)$. In such case, we obtain the gradient equation as:

$$\nabla F[q_2(\xi,t)] = -\left.\frac{J\lambda_4(\xi,\eta,t)}{C_p}\right|_{\eta=N} \tag{19}$$

7. Iterative procedure

The iterative procedure of the conjugate gradient method, as applied to the simultaneous estimation of $q_j(\xi,t)$, for $j=1,2$, is given by [34,35]:

$$q_j^{k+1}(\xi,t)=q_j^k(\xi,t)+\beta_j^k d_j^k(\xi,t),\quad j=1,2 \tag{20a}$$

where k is the number of iterations.

We used in this work Powell–Beale's version of the conjugate gradient method [39,41]. We also tested in this work the most common versions of the conjugate gradient method of Fletcher–Reeves and Polak–Ribiere [34,35,39]. However, for several test-cases they resulted in non-convergence of the iterative procedure because of the strong non-linear character of the physical problem under picture. As in Ref. [39], we found Powell–Beale's version of the conjugate gradient method more stable and robust than these two other versions. The directions

of descent for Powell–Beale's version of the conjugate gradient method, $d_j^k(\xi,t)$, are obtained from

$$d_j^k(\xi,t) = -\nabla F[q_j^k(\xi,t)] + \gamma_j^k d_j^{k-1}(\xi,t) + \chi_j^z d_j^z(\xi,t), \quad j = 1,2 \tag{20b}$$

where γ_j^k and χ_j^z are the conjugation coefficients. The superscript z in Eq. (20b) denotes the iteration number where a *restarting strategy* is applied to the iterative procedure of the Conjugate Gradient Method.

The conjugation coefficients γ_j^k and χ_j^z are given as [39,41]:

$$\gamma_j^k = \frac{\int_{\xi=1}^{M}\int_{t=0}^{t_f}\{\nabla F[q_j^k(\xi,t)] - \nabla F[q_j^{k-1}(\xi,t)]\}\nabla F[q_j^k(\xi,t)]\sqrt{b}J\,dt\,d\xi}{\int_{\xi=1}^{M}\int_{t=0}^{t_f}\{\nabla F[q_j^k(\xi,t)] - \nabla F[q_j^{k-1}(\xi,t)]\}d_j^{k-1}(\xi,t)\sqrt{b}J\,dt\,d\xi} \quad \text{for } k = 1,2,\ldots, \text{ with } \gamma_j^0 = 0 \text{ for } k = 0,\ j = 1,2 \tag{20c}$$

$$\chi_j^z = \frac{\int_{\xi=1}^{M}\int_{t=0}^{t_f}\{\nabla F[q_j^{z+1}(\xi,t)] - \nabla F[q_j^z(\xi,t)]\}\nabla F[q_j^k(\xi,t)]\sqrt{b}J\,dt\,d\xi}{\int_{\xi=1}^{M}\int_{t=0}^{t_f}\{\nabla F[q_j^{z+1}(\xi,t)] - \nabla F[q_j^z(\xi,t)]\}d_j^z(\xi,t)\sqrt{b}J\,dt\,d\xi} \quad \text{for } z = 1,2,\ldots, \text{ with } \chi_j^0 = 0 \text{ for } z = 0,\ j = 1,2 \tag{20d}$$

In accordance with Powell [41], the application of the conjugate gradient method with the conjugation coefficients given by Eqs. (20c) and (20d) requires restarting when gradients at successive iterations tend to be non-orthogonal (which is a measure of the local non-linearity of the problem) or when the direction of descent is not sufficiently downhill. Restarting is performed by making χ_j^z in Eq. (20b) equal to zero.

The non-orthogonality of gradients at successive iterations is tested by using:

$$\mathrm{ABS}\left[\int_{\xi=1}^{M}\int_{t=0}^{t_f}\nabla F[q_j^{k-1}(\xi,t)]\nabla F[q_j^k(\xi,t)]\sqrt{b}J\,dt\,d\xi\right] \geqslant 0.2\int_{\xi=1}^{M}\int_{t=0}^{t_f}\left\{\nabla F[q_j^k(\xi,t)]\right\}^2\sqrt{b}J\,dt\,d\xi \tag{21a}$$

where ABS(·) denotes the absolute value.

A non-sufficiently downhill direction of descent (i.e., the angle between the direction of descent and the negative gradient direction is too large) is identified if either of the following inequalities are satisfied:

$$-1.2\int_{\xi=1}^{M}\int_{t=0}^{t_f}\{\nabla F[q_j^k(\xi,t)]\}^2\sqrt{b}J\,dt\,d\xi \geqslant \int_{\xi=1}^{M}\int_{t=0}^{t_f}\{d_j^k(\xi,t)\nabla F[q_j^k(\xi,t)]\}\sqrt{b}J\,dt\,d\xi \geqslant -0.8\int_{\xi=1}^{M}\int_{t=0}^{t_f}\{\nabla F[q_j^k(\xi,t)]\}^2\sqrt{b}J\,dt\,d\xi \tag{21b}$$

We note that the coefficients 0.2, 1.2 and 0.8 appearing in Eqs. (21a) and (21b) are empirical and are the same used by Powell [41].

For the Powell–Beale's version of the Conjugate Gradient Method, the direction of descent given by Eq. (20b) is computed in accordance with the following algorithm for $k \geqslant 1$ [41]:

Step 1: Test the inequality (21a). If it is true set $z = k - 1$.
Step 2: Compute γ_j^k with Eq. (20c).
Step 3: If $k = z + 1$ set $\chi_j^z = 0$. If $k \neq z + 1$ compute χ_j^z with Eq. (20d).
Step 4: Compute the search direction $d_j^k(\xi,t)$ with Eq. (20b).
Step 5: If $k > z - 1$ test the inequalities (21b). If either one of them is satisfied set $z = k - 1$ and $\chi_j^z = 0$. Then recompute the search direction with Eq. (20b).

Expressions for the search step sizes β_j^k, for $j = 1, 2$, are obtained by minimizing $F[q_1^{k+1}(\xi,t), q_2^{k+1}(\xi,t)]$ with respect to β_1^k and β_2^k [34,35]. It results:

$$\beta_1^k = \frac{C_4C_5 - C_3C_1}{C_5C_2 - C_3^2}; \quad \beta_2^k = \frac{C_1C_2 - C_3C_4}{C_5C_2 - C_3^2} \tag{22a, b}$$

where:

$$C_1 = \int_{t=0}^{t_f}\sum_{s=1}^{S}[T(\mathbf{r}_s,t;q_1,q_2) - \mu_s(t)]\Delta T_2(\mathbf{r}_s,t;d_2^k)\,dt \tag{23a}$$

$$C_2 = \int_{t=0}^{t_f}\sum_{s=1}^{S}[\Delta T_1(\mathbf{r}_s,t;d_1^k)]^2\,dt \tag{23b}$$

$$C_3 = \int_{t=0}^{t_f}\sum_{s=1}^{S}\Delta T_1(\mathbf{r}_s,t;d_1^k)\Delta T_2(\mathbf{r}_s,t;d_2^k)\,dt \tag{23c}$$

$$C_4 = \int_{t=0}^{t_f}\sum_{s=1}^{S}[T(\mathbf{r}_s,t;q_1,q_2) - \mu_s(t)]\Delta T_1(\mathbf{r}_s,t;d_1^k)\,dt \tag{23d}$$

$$C_5 = \int_{t=0}^{t_f} \sum_{s=1}^{S} [\Delta T_2(\mathbf{r}_s, t; d_2^k)]^2 \, \mathrm{d}t \tag{23e}$$

In Eqs. (23a–e), $\Delta T_1(\mathbf{r}_s, t; d_1^k)$ and $\Delta T_2(\mathbf{r}_s, t; d_2^k)$ are the solutions of the sensitivity problems at the measurement locations $\mathbf{r}_s = (\xi_s, \eta_s)$, given by Eqs. (7a–e) for $j = 1, 2$, respectively, obtained by setting $\Delta q_j(\xi, t) = d_j^k(\xi, t)$.

8. Stopping criterion

The iterative procedure of the conjugate gradient method is not capable of providing by itself regularized solutions for inverse problems. In fact, it is generally observed that the random errors present on the measured variables are amplified for the solution of the inverse problem, as a result of its ill-posed character, when estimated temperatures approach the measured ones during the minimization of the functional (5). However, the use of the conjugate gradient method may result on stable solutions if the *Discrepancy Principle* [34] is used to specify the tolerance for the stopping criterion of the iterative procedure. In the Discrepancy Principle, the solution is assumed to be sufficiently accurate when the difference between measured and estimated tempera-

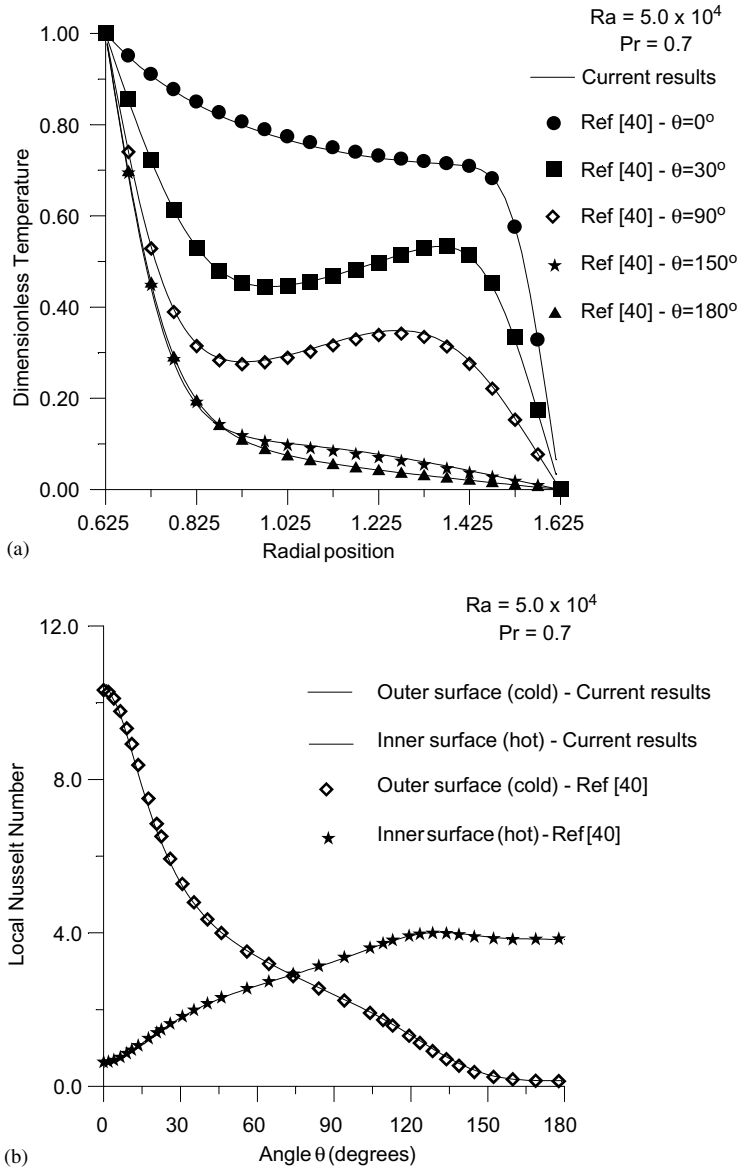

Fig. 2. Comparison between current and benchmark results for (a) temperature and (b) Nusselt number.

tures is of the order of magnitude of the measurement errors, that is,

$$|T[\xi_s, \eta_s, t; q_1(\xi,t), q_2(\xi,t)] - \mu_s(t)| \approx \sigma \tag{24}$$

where σ is the standard deviation of the measurements, which is assumed constant in the present analysis.

The stopping criterion used here is given by

$$F[q_1(\xi,t), q_2(\xi,t)] < \varepsilon \tag{25}$$

where $F[q_1(\xi,t), q_2(\xi,t)]$ is computed with Eq. (5). The tolerance ε based on the Discrepancy Principle is then obtained by substituting Eq. (24) into Eq. (5). It results:

$$\varepsilon = \frac{1}{2} S \sigma^2 t_f \tag{26}$$

For cases involving errorless measurements, stable solutions for the inverse problem can be obtained by

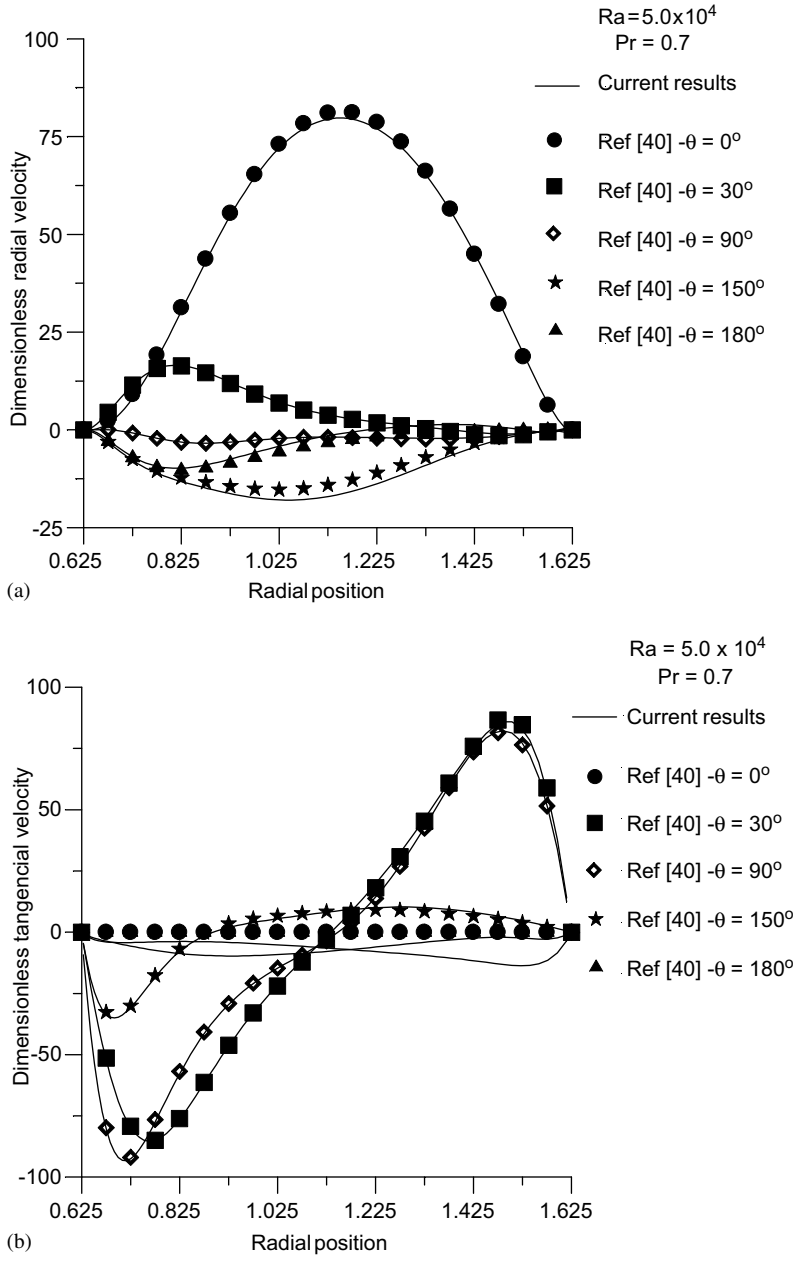

Fig. 3. Comparison between current and benchmark results for (a) radial velocity and (b) tangential velocity.

specifying the tolerance ε as a small number, since no perturbation is present in the input (measured) data. However, such is the case only if the sensors are appropriately located in regions where the measurements are sufficiently sensitive to variations in the unknown function.

The conjugate gradient method, as applied to the estimation of the unknown functions $q_j(\xi,t)$, $j=1,2$, can be arranged in a computational algorithm, which can be readily adapted from those found in Ref. [35].

9. Results and discussion

9.1. Validation of the direct problem

We now turn our attention to the annular circular cavity depicted in Fig. 1. The results obtained here for natural convection of air were compared to those of Pereira et al. [40] obtained with the Generalized Integral Transform Technique. The physical properties were taken as: $\rho = 1.19$ kg/m^3; $\mu = 1.8\times10^{-5}$ kg/m s; $\beta = 0.00341$ K^{-1}; $Pr = 0.70$; $K = 0.2624$ W/m K; $C_p = 1020.4$ J/kg °C. The test-cases analyzed below correspond to a Rayleigh number of 5×10^4, where the characteristic length used was $L = R_2 - R_1$. For this Rayleigh number, R_2 was taken as 54.4 mm and R_1 as 22.9 mm, while the temperatures at the walls $\eta = N$ and $\eta = 1$ were taken as $T_h = 30$ °C and $T_c = 20$ °C, respectively. The Rayleigh number was defined as:

$$Ra_L = \frac{\rho g\beta(T_h - T_c)L^3}{\mu\alpha} \tag{27}$$

Figs. 2 and 3 show a comparison between the current and the benchmark [40] results for the steady-state dimensionless temperature, Nusselt number at the inner and outer walls, radial and tangential velocities, respectively, for the test-case analyzed here. The dimensionless variables presented in these figures are defined as:

$$v_r = \frac{V_R L}{\alpha}, \quad v_\theta = \frac{V_\Theta L}{\alpha}, \quad r = \frac{R}{L},$$
$$\Theta = \frac{T - T_c}{T_h - T_c}, \quad Pr = \frac{\mu C_p}{K} \tag{28a–e}$$

For the current numerical results shown in Figs. 2 and 3, a finite-volume grid was used with 80×80 cells. Figs. 2 and 3 show that the present numerical results are in excellent agreement with those of Ref. [40]. However, some deviations can be observed at $\theta = 0°$ and $\theta = 180°$ for the tangential velocity. Such deviations are due to the fact that the current grid did not have enough cells to capture the velocity at these locations and the numerical results are shifted of 1°.

9.2. Inverse problem

We will consider in this section the solution of the inverse problem involving the same direct problem for which the numerical solution was validated in the previous section. Therefore, the heat fluxes to be estimated are those required to maintain the surfaces $\eta = 1$ and $\eta = N$ at the constant temperatures $T_c = 20$ °C and $T_h = 30$ °C, respectively. The initial temperature was taken as $T_c = 20$ °C. As a result, the unknown heat fluxes vary along the surfaces $\eta = 1$ and $\eta = N$, as well as in time.

We use simulated temperature measurements for the solution of the present inverse problem. These measurements are obtained from the solution of the direct problem for known boundary heat fluxes $q_1(\xi,t)$ and $q_2(\xi,t)$, at the surfaces $\eta = 1$ and $\eta = N$, respectively. The measurements obtained in such a manner are considered as *exact* ($\mu_{s,ex}(t)$) and, in order to simulate measurement errors, a random term is added to them in the form:

$$\mu_s(t) = \mu_{s,ex}(t) + \omega\sigma \tag{29}$$

where ω is a random variable with normal distribution, zero mean and unitary standard deviation and σ is the standard deviation of the measurement errors.

We examined in this work several test-cases involving different numbers and positions of sensors, as well as different levels of simulated random measurement errors. Table 1 summarizes such test-cases and the RMS errors for each of the estimated functions. The RMS error is defined as:

Table 1
Test cases for the inverse problem

Test-case	Depth below the surface $\eta = 1$ (mm)	Depth below the surface $\eta = N$ (mm)	Number of sensors	σ (°C)	ε_{RMS} (W/m^2) $\eta = 1$	ε_{RMS} (W/m^2) $\eta = N$
1	0.38	0.13	80	0.00	0.55	5.49
2	0.38	0.13	27	0.00	0.69	7.26
3	0.38	0.13	4	0.00	0.90	6.44
4	0.38	0.68	4	0.00	1.20	10.22
5	1.08	1.25	4	0.00	2.51	13.06
6	1.77	1.83	4	0.00	4.09	14.58
7	1.08	1.25	27	0.6	6.33	14.90

$$\varepsilon_{\mathrm{RMS},j}=\sqrt{\frac{1}{(M-1)I}\sum_{m=1}^{M-1}\sum_{i=1}^{I}[q_{\mathrm{ex},j}(\xi_m,t_i)-q_{\mathrm{est},j}(\xi_m,t_i)]^2}$$

for $j=1,2$. (30)

Test-cases 1–6 involve the use of errorless ($\sigma=0$) measurements in the inverse analysis, while test-case 7 involve the use of measurements of standard deviation $\sigma=0.6$ °C. Since the measurement errors are assumed to be additive, uncorrelated and normally distributed, with zero mean and constant standard deviation, at the 99% confidence level the measurement errors are at most 1.6 °C in magnitude. For all test-cases we have assumed available measurements every 0.005 s (200 Hz) for each sensor and the final time was taken as 40 s. The initial guesses were taken as $q_1(\xi,t)=q_2(\xi,t)=0.1$ W/m^2. By examining Eqs. (13e), (18b) and (19), we can notice that the gradient of the functional is null at the final time

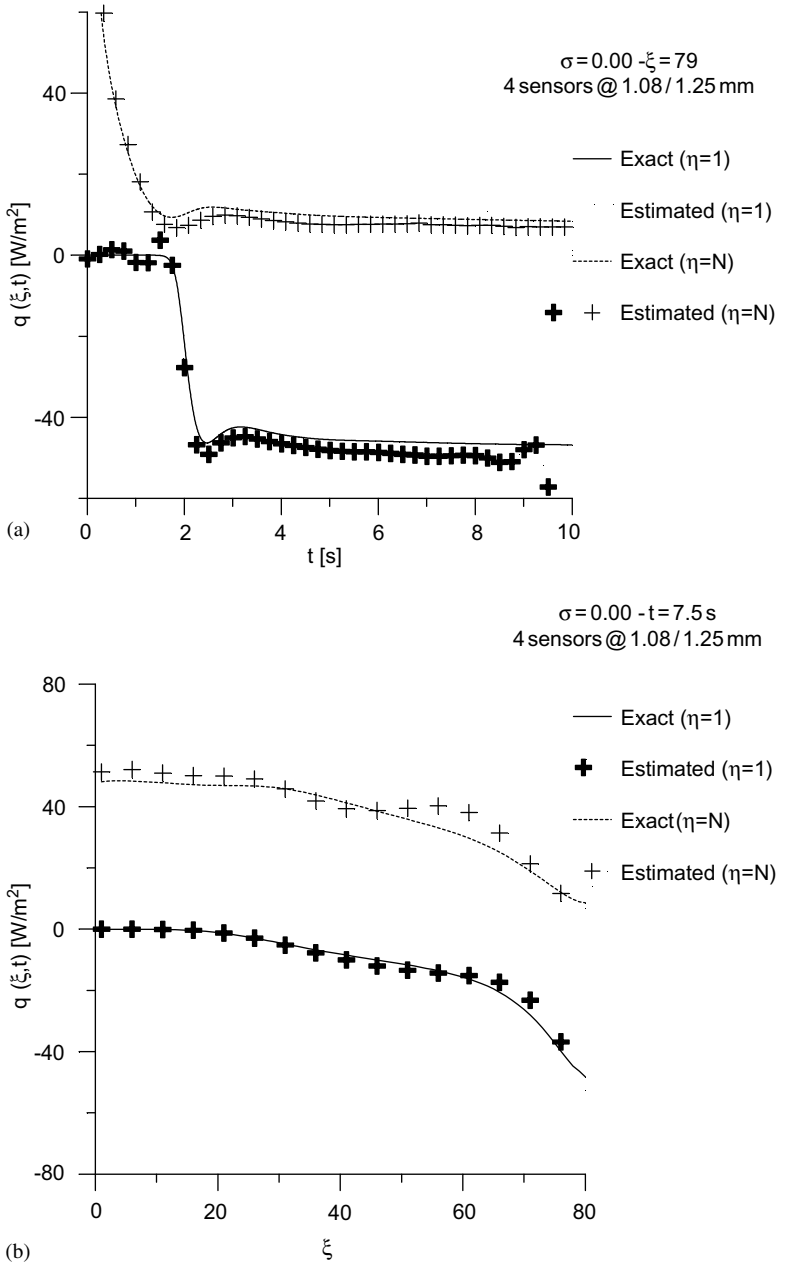

Fig. 4. Results for test-case 5: (a) $\xi=79$, (b) $t=7.5$ s.

$t = t_f$. Therefore, the initial guesses used for $q_1(\xi, t)$ and $q_2(\xi, t)$ at $t = t_f$ are never changed by the iterative procedure of the conjugate gradient method. As a result, oscillations may appear in the solution in the neighborhood of the final time, if the initial guesses are too different from the exact solutions. Thus, a final time larger than that of interest was used in the analysis, so that the effects of the initial guesses were not noticeable in the time domain that the solution was sought.

Since the numbers of sensors in test-cases 2–7 were smaller than the number of control volumes used for the discretization, an interpolation procedure was used for the measured temperatures along the ξ direction. NETLIB's subroutine GCVSPL, based on the cross-

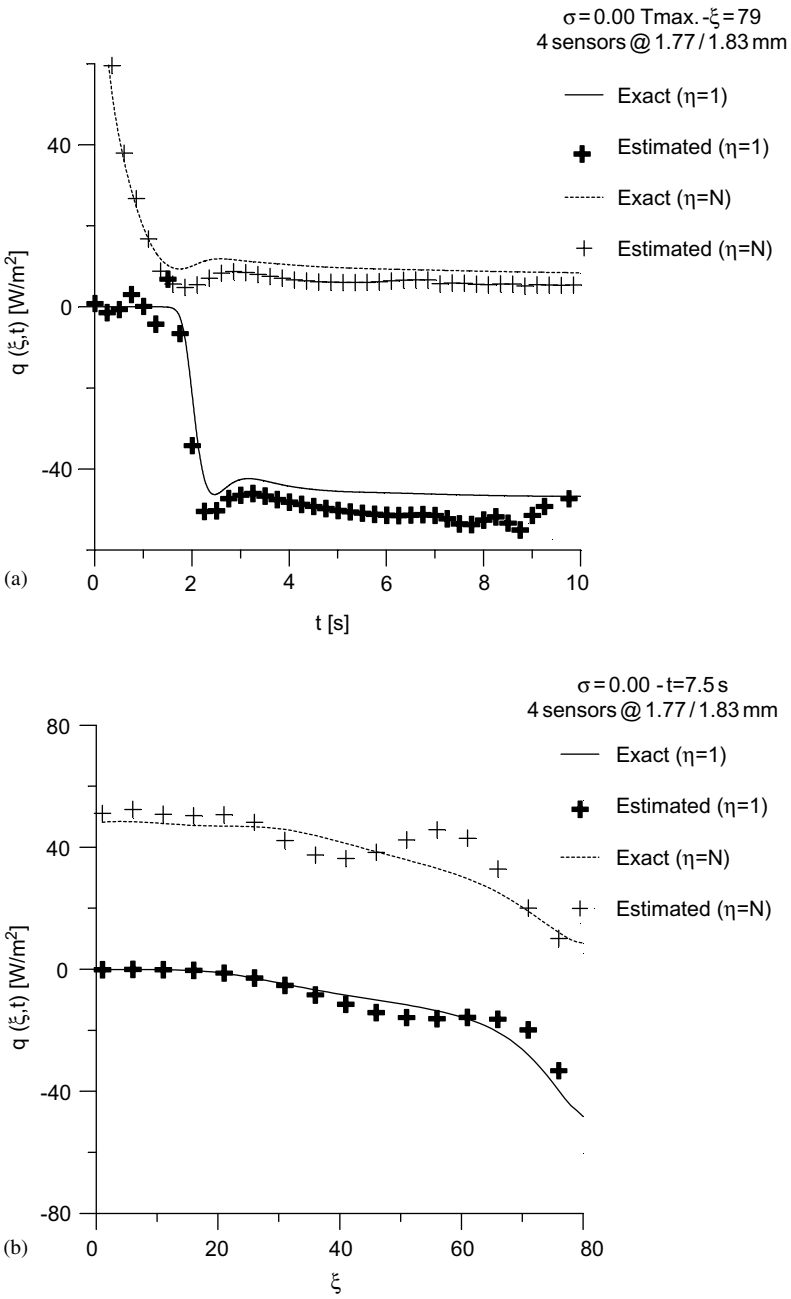

Fig. 5. Results for test-case 6: (a) $\xi = 79$, (b) $t = 7.5$ s.

validation smoothing procedure, was used for the interpolation. The sensors were assumed to be evenly located along the ξ direction, near each of the boundaries with unknown flux.

Test-case 1 represents an ideal case where there is one sensor at each control volume next to the surfaces $\eta = 1$ and $\eta = N$ (0.38 mm below the surface at $\eta = 1$ and 0.13 mm below the surface at $\eta = N$). This test-case gives the minimum RMS error for the grid size used for the current simulation. Note in Table 1 that, as we decrease the number of sensors from 80 in test-case 1 to 4 in test-case 3, the RMS error increases since less information is available from the measurements inside the cavity. Similarly, the RMS error increases when the sensors are located deeper inside the cavity, as we can notice by comparing test-cases 3 and 4 in Table 1.

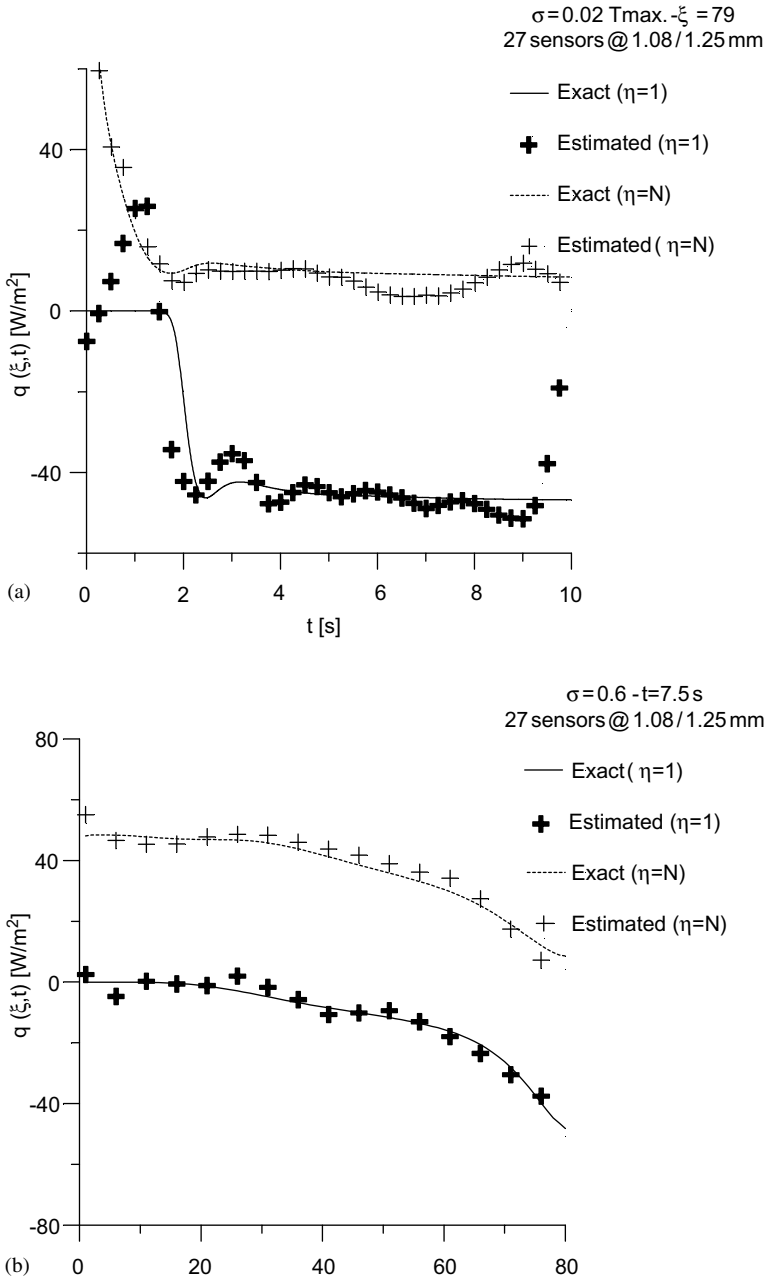

Fig. 6. Results for test-case 7: (a) $\xi = 79$, (b) $t = 7.5$ s.

Fig. 4a and b present the results for test-case 5, where four sensors were located 1.08 mm below the surface at $\eta = 1$ and four sensors were located 1.25 mm below the surface at $\eta = N$. These figures show that quite accurate results can be obtained with only four sensors located about 1 mm below each surface, for the physical problem considered in this paper. Note in Fig. 4a that the exact functions are underestimated at $\xi = 79$ after $t = 2$ s; also note in Fig. 4b that the estimated functions tend to oscillate about the exact ones for $t = 7.5$ s. However, the sharp variation of the heat flux at $\eta = 1$ around 2 s is accurately captured, as illustrated in Fig. 4a.

The accuracies of the estimated functions deteriorate if the sensors are located deeper into the cavity, as illustrated in Fig. 5a and b, which present the results obtained for test-case 6. For such test-case, four sensors were located about 1.8 mm below each of the surfaces. In fact, no accurate results could be obtained with sensors farther than 1.8 mm from the surfaces with unknown fluxes, because they were located outside the thermal boundary layers and, therefore, were not sensitive to variations in the boundary heat fluxes.

We now examine the results obtained for test-case 7, with measurements containing random errors of standard deviation $\sigma = 0.6$ °C. For test-case 7, the measurements of 27 sensors located near each of the boundaries were assumed available for the inverse analysis. The sensors were located 1.08 mm below the surface at $\eta = 1$ and 1.25 mm below the surface at $\eta = N$. Fig. 6a and b show that the estimated functions are in very good agreement with the exact ones for such test-case, although some oscillations are observed in the inverse problem solution, specially near the sharp variation around 2 s at $\eta = N$ (see Fig. 6a).

10. Conclusions

In this paper we applied the conjugate gradient method with adjoint problem for the simultaneous identification of two boundary heat fluxes in a natural convection problem in an irregular cavity. A function estimation approach was utilized, where no information was assumed available regarding the functional form of the unknowns. The more involved inverse problem concerned with the estimation of position- and time-dependent functions was examined. Direct and inverse problems were formulated in terms of generalized coordinates. Therefore, the present solution procedure can readily be applied to cavities with different geometries.

Results obtained with simulated temperature measurements reveal that quite accurate estimates can be obtained for the unknown functions with the present inverse problem approach. However, the sensors need to be located near each of the surfaces, inside the thermal boundary layer, in order to be sensitive to variations on the boundary heat flux.

Acknowledgements

The first author is grateful for the doctoral fellowship provided by CNPq, the Brazilian Council for Scientific and Technological Development, during the years of 1998 through 2001. The CPU time for this work was provided by NACAD-UFRJ (Cray-J90) and CESUP-UFRGS (Cray-T94). This work was partially funded by the CNPq grant 522.469/94-9 and by the FAPERJ grant E-26/170.344/2000.

References

[1] A. Moutsoglou, An inverse convection problem, J. Heat Transfer 111 (1989) 37–43.
[2] A. Moutsoglou, Solution of an elliptic inverse convection problem using a whole domain regularization technique, J. Thermophys. 4 (1990) 341–349.
[3] C.H. Huang, M.N. Özisik, Inverse problem of determining unknown wall heat flux in laminar flow through a parallel plate duct, Numer. Heat Transfer, Part A 21 (1992) 55–70.
[4] R. Raghunath, Determining entrance conditions from downstream measurements, Int. Commun. Heat Mass Transfer 20 (1993) 173–183.
[5] J.C. Bokar, M.N. Özisik, Inverse analysis for estimating the time varying inlet temperature in laminar flow inside a parallel plate duct, Int. J. Heat Mass Transfer 38 (1995) 39–45.
[6] F.B. Liu, M.N. Özisik, Inverse analysis of transient turbulent forced convection inside parallel plates, Int. J. Heat Mass Trasnfer 39 (1996) 2615–2618.
[7] F.B. Liu, M.N. Özisik, Estimation of inlet temperature profile in laminar duct flow, Inverse Problems Eng. 3 (1996) 131–141.
[8] H.A. Machado, H.R.B. Orlande, Estimation of the timewise and spacewise variation of the wall heat flux to a non-newtonian fluid in a parallel plate channel, in: Proc. of the Int. Symp. on Transient Convective Heat Transfer, Cesme, Turkey, August 1996, pp. 587–596.
[9] H.A. Machado, H.R.B. Orlande, Inverse analysis for estimating the timewise and spacewise variation of the wall heat flux in a parallel plate channel, Int. J. Numer. Methods Heat Fluid Flow 7 (1997) 696–710.
[10] H.A. Machado, H.R.B. Orlande, Inverse problem for estimating the heat flux to a non-newtonian fluid in a parallel plate channel, J. Braz. Soc. Mech. Sci. XX (1998) 51–61.
[11] I. Szczygiet, Estimation of the boundary conditions in convectional heat transfer problems, in: Proc. of the 32nd National Heat Transfer Conference, ASME HTD Vol. 340, vol. 2, 1997, Baltimore, pp. 17–23.
[12] S. Moaveni, An inverse problem involving thermal energy equation, in: Proc. of the 32nd National Heat Transfer

Conference, ASME HTD Vol. 340, vol. 2, 1997, Baltimore, pp. 49–54.
[13] J.B. Aparecido, M.N. Özisik, Nonlinear parameter estimation in laminar forced convection inside a circular tube, in: Proc. of the 3rd International Conference on Inverse Problems, Port Ludlow, June 1999, pp. 283–294.
[14] M.J. Colaço, H.R.B. Orlande, A function estimation approach for the identification of the transient inlet profile in parallel plate channels, in: M. Tanaka, G. Dulikravich (Eds.), Inverse Problems in Engineering Mechanics II, International Symposium on Inverse Problems in Engineering Mechanics, Nagano City, Japan, 2000, pp. 409–418.
[15] C.H. Huang, W.W. Chen, A three-dimensional inverse forced convection problem in estimating surface heat flux by conjugate gradient method, Int. J. Heat Mass Transfer 43 (2000) 3171–3181.
[16] G.Z. Yang, N. Zabaras, An adjoint method for the inverse design of solidification process with natural convection, Int. J. Numer. Methods Eng. 42 (1998) 1121–1144.
[17] N. Zabaras, T.H. Nguyen, Control the freezing interface morphology in solidification processes in the presence of natural convection, Int. J. Numer. Methods Eng. 38 (1995) 1555–1578.
[18] N. Zabaras, G.Z. Yang, A functional optimization formulation and implementation of an inverse natural convection problem, Comput. Methods Appl. Mech. Eng. 144 (1997) 245–274.
[19] M. Prud'homme, T. Nguyen, Whole time domain approach to the inverse natural convection problem, Numer. Heat Transfer, Part A 32 (1997) 169–186.
[20] H.M. Park, O.Y. Chung, Inverse natural convection problem of estimating wall heat flux using a moving sensor, J. Heat Transfer 121 (1999) 528–536.
[21] H.M. Park, O.Y. Chung, An inverse natural convection problem of estimating the strength of a heat source, Int. J. Heat Mass Transfer 42 (1999) 4259–4273.
[22] H.M. Park, O.Y. Chung, On the solution of an inverse natural convection problem using various conjugate gradient methods, Int. J. Numer. Methods Eng. 47 (2000) 821–842.
[23] H.M. Park, O.Y. Chung, Inverse natural convection problem of estimating wall heat flux, Chem. Eng. Sci. 55 (2000) 2131–2141.
[24] Z.R. Li, M. Prud'homme, T.H. Nguyen, A numerical solution for the inverse natural-convection problem, Numer. Heat Transfer, Part B 28 (1995) 307–321.
[25] C. Gonçalves, L. Silva, A. Neto, D. Rade, G. Guimarães, An inverse technique applied to natural convection over a heated vertical plate, in: Proc. of the 34nd ASME National Heat Transfer Conference, Paper NHTC2000-12311, Pittsburg, August 20–22, 2000.
[26] M.J. Colaço, H.R.B. Orlande, Inverse problem of simultaneous estimation of two boundary heat fluxes in parallel plate channels, J. Braz. Soc. Mech. Sci. XXIII (2001) 201–215.
[27] M.J. Colaço, H.R.B. Orlande, Inverse forced convection problem of simultaneous estimation of two boundary heat fluxes in irregularly shaped channels, Numer. Heat Transfer, Part A—Appl. 39 (2001) 737–760.
[28] M.J. Colaço, H.R.B. Orlande, A natural convection inverse problem of simultaneous estimation of two boundary heat fluxes in rectangular cavities, Paper 0465, 12th International Heat Transfer Conference, Grenoble, August 2003.
[29] C.-H. Huang, C.-Y. Yeh, An optimal control algorithm for entrance concurrent flow problems, Int. J. Heat Mass Transfer 46 (2003) 1013–1027.
[30] J. Su, A. Silva Neto, Simultaneous estimation of inlet temperature and wall heat flux in turbulent circular pipe flow, Numer. Heat Transfer, Part A—Appl. 40 (2001) 751–766.
[31] M. Prud'homme, S. Jasmin, Determination of a heat source in porous medium with convective mass diffusion by an inverse method, Int. J. Heat Mass Transfer 46 (2003) 2065–2075.
[32] Manuel Girault, Daniel Petit, François Penot, Identification of velocity distribution in a turbulent flow inside parallel-plate ducts from wall temperature measurements, in: H.R.B. Orlande (Ed.), Inv. Problems in Engineering: Theory and Practice, vol. 2, e-papers, Rio de Janeiro, 2002, pp. 195–202.
[33] J.V. Beck, B. Blackwell, C.R.St. Clair, Inverse Heat Conduction: Ill-Posed Problems, Wiley Inters, New York, 1985.
[34] O.M. Alifanov, Inverse Heat Transfer Problems, Springer-Verlag, New York, 1994.
[35] M.N. Özisik, H.R.B. Orlande, Inverse Heat Transfer: Fundamentals and Applications, Taylor & Francis, New York, 2000.
[36] J.F. Thompson, Z.U.A. Warsi, C.W. Mastin, Numerical Grid Generation, North-Holland, New York, 1987.
[37] G.D. Raithby, K.E. Torrance, Upstream-weighted differencing schemes and their applications to elliptic problems involving fluid flow, Comput. Fluids 2 (1974) 191–206.
[38] J.P. Van Doormal, G.D. Raithby, Enhancements of the simple method for predicting incompressible fluid flow, Numer. Heat Transfer 7 (1984) 147–163.
[39] M.J. Colaço, H.R.B. Orlande, A comparison of different versions of the conjugate gradient method of function estimation, Numer. Heat Transfer, Part A—Appl. 36 (1999) 229–249.
[40] L.M. Pereira, R.M. Cotta, J.S. Pérez-Guerrero, Forced and natural convection in annular concentric channels and cavities by integral transforms, in: Proc. of the 8th Brazilian Congress of Thermal Engineering and Sciences, Porto Alegre, Brazil, October 2000.
[41] M.J.D. Powell, Restart procedures for the conjugate gradient method, Math. Program. 12 (1977) 241–254.